

Manipulating Topological Edge Spins in a One-Dimensional Optical Lattice

Xiong-Jun Liu,^{1,2,3} Zheng-Xin Liu,^{4,5} and Meng Cheng²

¹Joint Quantum Institute, Department of Physics, University of Maryland, College Park, Maryland 20742, USA

²Condensed Matter Theory Center, Department of Physics, University of Maryland, College Park, Maryland 20742, USA

³Department of Physics, Institute for Advanced Study, Hong Kong University of Science and Technology, Clear Water Bay, Hong Kong

⁴Institute for Advanced Study, Tsinghua University, Beijing 100084, People's Republic of China

⁵Department of Physics, Massachusetts Institute of Technology, Cambridge, Massachusetts 02139, USA

(Received 8 October 2012; published 12 February 2013)

We propose to observe and manipulate topological edge spins in a one-dimensional optical lattice based on currently available experimental platforms. Coupling the atomic spin states to a laser-induced periodic Zeeman field, the lattice system can be driven into a symmetry protected topological (SPT) phase, which belongs to the chiral unitary (AIII) class protected by particle number conservation and chiral symmetries. In the free-fermion case the SPT phase is classified by a Z invariant which reduces to Z_4 with interactions. The zero edge modes of the SPT phase are spin polarized, with left and right edge spins polarized to opposite directions and forming a topological spin qubit (TSQ). We demonstrate a novel scheme to manipulate the zero modes and realize single spin control in an optical lattice. The manipulation of TSQs has potential applications to quantum computation.

DOI: 10.1103/PhysRevLett.110.076401

PACS numbers: 71.10.Pm, 37.10.Jk, 42.50.Ex, 71.70.Ej

Introduction.—Since the discovery of the quantum Hall effect in a two-dimensional electron gas [1], the search for nontrivial topological states has become an exciting pursuit in condensed matter physics [2]. The recently observed time-reversal invariant topological insulators have opened a new chapter in the study of topological phases (TPs), attracting great efforts in both theory and experiments [3,4]. Depending on whether the ground states have long-range or short-range entanglement, the TPs can be classified into intrinsic or symmetry-protected topological (SPT) orders [5–7]. Being protected by the bulk gap, the intrinsic TPs are robust against any local perturbations, and the SPT phases are robust against those respecting given symmetries [5–8]. This property may be applied to fault-tolerant quantum computation [9].

While in theory there are numerous types of TPs, existing topological orders in nature are rare. The recent great advancement in realizing an effective spin-orbit (SO) interaction in cold atoms [10–15] opens intriguing new possibilities to probe SO effects [16] and TPs in a controllable fashion. Theoretical proposals have been introduced in cold atoms for the study of topological insulators [17–21] and topological superfluids [22–26]. Experimental studies of these exotic phases are, however, a delicate issue due to stringent conditions such as complicated lattice configurations or SO interactions. By far the only experimentally realized SO interaction [11–15] is the equal-Rashba-Dresselhaus-type SO term as theoretically proposed by Liu *et al.* [10]. Therefore, how to observe nontrivial topological states with currently available experimental platforms is a central issue in the field of cold atoms [25].

In this Letter, we propose to observe and manipulate topological edge spins in a one-dimensional (1D) optical

lattice with the SO interaction realizable in recent experiments [11–14]. The predicted SPT phase belongs to the AIII class and is protected by $U(1)$ and chiral symmetries, with spin-polarized zero modes forming topological spin qubits (TSQs). Our results may open the way to observe topological states of all ten Altland-Zirnbauer symmetry classes [5] with realistic cold atom systems, and may have a broad range of applications including realizing single spin control in an optical lattice.

Model.—Our model is based on quasi-1D cold fermions trapped in an optical lattice, with the internal three-level Λ -type configuration coupled to radiation, as shown in Fig. 1. The transitions $|g_1\rangle, |g_2\rangle \rightarrow |e\rangle$ are driven by the laser fields with Rabi frequencies $\Omega_1(x) = \Omega_0 \sin(k_0x/2)$ and $\Omega_2(x) = \Omega_0 \cos(k_0x/2)$, respectively. In the presence of a large one-photon detuning $|\Delta| \gg \Omega_0$ and a small two-photon detuning $|\delta| \ll \Omega_0$ for the transitions [see Fig. 1(a)], the Hamiltonian of the light-atom coupling

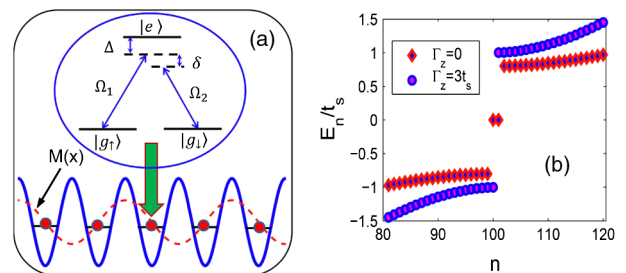


FIG. 1 (color online). (a) Cold fermions trapped in a 1D optical lattice with an internal three-level Λ -type configuration coupled to radiation. (b) Energy spectra with open boundary condition in the topological (diamond, $\Gamma_z = 0$) and trivial (circle, $\Gamma_z = 3t_s$) phases. The SO coupled hopping $t_{so}^{(0)} = 0.4t_s$.

system reads $H = H_0 + H_1$, with $H_0 = \sum_{\sigma=\uparrow,\downarrow} [V_{\sigma}^2 + V_{\sigma}(x)] |g_{\sigma}\rangle\langle g_{\sigma}| + \hbar\delta |g_{\uparrow}\rangle\langle g_{\downarrow}|$, $H_1 = \hbar\Delta |e\rangle\langle e| - \hbar(\Omega_1 |e\rangle\langle g_{\uparrow}| + \Omega_2 |e\rangle\langle g_{\downarrow}| + \text{H.c.})$. Here the diagonal potentials $V_{\uparrow,\downarrow}(x)$ are used to construct the 1D optical lattice, and $\sigma_{y,z}$ are the Pauli matrices in spin space. For $|\Delta| \gg \Omega_0$, the lasers $\Omega_{1,2}$ induce a two-photon Raman transition between $|g_{\uparrow}\rangle$ and $|g_{\downarrow}\rangle$. This configuration has been used to create the equal-Rashba-Dresselhaus SO interaction [10–15]. The effect of the small two-photon detuning is equivalent to a Zeeman field along the z axis $\Gamma_z = \hbar\delta/2$, which in experiments can be precisely controlled with an acoustic-optic modulator. Eliminating the excited state by $|e\rangle \approx \frac{1}{\Delta}(\Omega_1^* |g_{\uparrow}\rangle + \Omega_2^* |g_{\downarrow}\rangle)$ yields the effective Hamiltonian

$$H_{\text{eff}} = \frac{p_x^2}{2m} + \sum_{\sigma=\uparrow,\downarrow} [V_{\sigma}^{\text{Latt}}(x) + \Gamma_z \sigma_z] |g_{\sigma}\rangle\langle g_{\sigma}| - [M(x) |g_{\uparrow}\rangle\langle g_{\downarrow}| + \text{H.c.}], \quad (1)$$

where $M(x) = M_0 \sin(k_0 x)$ with $M_0 = \frac{\hbar\Omega_0^2}{2\Delta}$ representing a transverse Zeeman field induced by the Raman process.

We next derive the tight-binding model. We consider first the s -band model in an optical lattice formed by the trapping potentials $V_{\uparrow,\downarrow}^{\text{Latt}}(x) = -V_0 \cos^2(k_0 x)$, with the lattice trapping frequency $\omega = (2V_0 k_0^2/m)^{1/2}$ [27]. From the even parity of the local s orbitals $\phi_{s\sigma}$ ($\sigma = \uparrow, \downarrow$), the periodic term $M(x)$ does not couple the intrasite orbitals $\phi_{s\uparrow}^{(i)}$, but leads to a spin-flip hopping by $t_{s\sigma}^{ij} = \int dx \phi_{s\uparrow}^{(i)}(x) M(x) \phi_{s\downarrow}^{(j)}(x)$ [see Fig. 1(a)], representing the induced SO interaction. The spin-conserved hopping reads $t_s = \int dx \phi_{s\sigma}^{(j)}(x) [\frac{p_x^2}{2m} + V] \phi_{s\sigma}^{(j+1)}(x)$. Bearing these results in mind we write down the effective Hamiltonian in the tight-binding form: $H = -t_s \sum_{\langle i,j \rangle, \sigma} \hat{c}_{i\sigma}^{\dagger} \hat{c}_{j\sigma} + \sum_i \Gamma_z (\hat{n}_{i\uparrow} - \hat{n}_{i\downarrow}) + [\sum_{\langle i,j \rangle} t_{s\sigma}^{ij} \hat{c}_{i\uparrow}^{\dagger} \hat{c}_{j\downarrow} + \text{H.c.}]$, with $\hat{n}_{i\sigma} = \hat{c}_{i\sigma}^{\dagger} \hat{c}_{i\sigma}$. It can be verified that $t_{s\sigma}^{i,j\pm 1} = \pm (-1)^j t_{s\sigma}^{(0)}$, where $t_{s\sigma}^{(0)} = \frac{\Omega_0^2}{\Delta} \int dx \phi_{s\sigma}(x) \sin(2k_0 x) \phi_{s\sigma}(x - a)$ with a the lattice constant. Redefining the spin-down operator $\hat{c}_{j\downarrow} \rightarrow e^{i\pi x_j/a} \hat{c}_{j\downarrow}$, we recast the Hamiltonian into

$$H = -t_s \sum_{\langle i,j \rangle} (\hat{c}_{i\uparrow}^{\dagger} \hat{c}_{j\uparrow} - \hat{c}_{i\downarrow}^{\dagger} \hat{c}_{j\downarrow}) + \sum_i \Gamma_z (\hat{n}_{i\uparrow} - \hat{n}_{i\downarrow}) + \left[\sum_j t_{s\sigma}^{(0)} (\hat{c}_{j\uparrow}^{\dagger} \hat{c}_{j+1\downarrow} - \hat{c}_{j\downarrow}^{\dagger} \hat{c}_{j-1\downarrow}) + \text{H.c.} \right]. \quad (2)$$

The above model can also be realized with p -band fermions in a different configuration of the optical lattice, $V_{\uparrow,\downarrow}^{\text{Latt}}(x) = -V_0 \sin^2(k_0 x)$, which can be directly verified by noticing the odd parity of the p orbitals. Remarkably, for the p -band model the periodic Zeeman term $M(x)$ and the 1D lattice can be realized *simultaneously* by setting $\Omega_1(x) = \Omega_0 \sin(k_0 x)$ and $\Omega_2 = \Omega_0$ without applying additional lasers (see the Supplemental Material [28] for details). This further greatly simplifies the experimental

setup and we believe that our proposal can be realized with realistic experimental platforms.

We analyze the symmetry of the Hamiltonian [Eq. (2)]. The time-reversal and charge conjugation operators are respectively defined by $\mathcal{T} = iK\sigma_y$ with K the complex conjugation, and \mathcal{C} : $(\hat{c}_{\sigma}, \hat{c}_{\sigma}^{\dagger}) \mapsto (\sigma z)_{\sigma\sigma'} (\hat{c}_{\sigma'}^{\dagger}, \hat{c}_{\sigma'})$. One can check that while both \mathcal{T} and \mathcal{C} are broken in H , the chiral symmetry, defined as their product, is respected and $(\mathcal{C}\mathcal{T})H(\mathcal{C}\mathcal{T})^{-1} = H$, with $(\mathcal{C}\mathcal{T})^2 = 1$. Note that the chiral symmetry is still preserved if a Zeeman term $\Gamma_y \sigma_y$ along the y axis is included in H . The complete symmetry group then reads $U(1) \times Z_2^T$, where $U(1)$ gives particle-number conservation and the antiunitary group Z_2^T is formed by $\{I, \mathcal{C}\mathcal{T}\}$. The SPT phase of our free-fermion system belongs to the chiral unitary (AIII) class and is characterized by a Z invariant [5–7]. H can be rewritten in k space as $H = -\sum_{k,\sigma\sigma'} \hat{c}_{k,\sigma}^{\dagger} [d_z(k)\sigma_z + d_y(k)\sigma_y]_{\sigma,\sigma'} \hat{c}_{k,\sigma'}$, with $d_y = 2t_{s\sigma}^{(0)} \sin(ka)$ and $d_z = -\Gamma_z + 2t_s \cos(ka)$. This Hamiltonian describes a nontrivial topological insulator for $|\Gamma_z| < 2t_s$ and otherwise a trivial insulator, with the bulk gap $E_g = \min\{|2t_s - |\Gamma_z||, 2|t_{s\sigma}^{(0)}|\}$ [see Fig. 1(b)]. In particular, when $\Gamma_{y,z} = 0$ and $t_s = |t_{s\sigma}^{(0)}|$, our model gives rise to a flat band with a nontrivial topology.

Edge states.—The nontrivial topology can support degenerate boundary modes. Considering hard wall boundaries located at $x = 0, L$, respectively, [29] and diagonalizing H in position space $H = \sum_{x_i} \mathcal{H}(x_i)$ with $\mathcal{H}(x_i) = -(t_s \sigma_z + i t_{s\sigma}^{(0)} \sigma_y) \hat{c}_{x_i}^{\dagger} \hat{c}_{x_i+a} + \Gamma_z \sigma_z \hat{c}_{x_i}^{\dagger} \hat{c}_{x_i} + \text{H.c.}$, we obtain the edge state localized on the left boundary $x = 0$ as

$$\psi_L(x_i) = \frac{1}{\sqrt{\mathcal{N}}} [(\lambda_+)^{x_i/a} - (\lambda_-)^{x_i/a}] |\chi_+\rangle, \quad (3)$$

and accordingly the one on $x = L$ by $\psi_R(x_i) = \frac{1}{\sqrt{\mathcal{N}}} [(\lambda_+)^{(L-x_i)/a} - (\lambda_-)^{(L-x_i)/a}] |\chi_-\rangle$. Here \mathcal{N} is the normalization factor, the spin eigensates $\sigma_x |\chi_{\pm}\rangle = \pm |\chi_{\pm}\rangle$, and $\lambda_{\pm} = (\Gamma_z \pm \sqrt{\Gamma_z^2 - 4t_s^2 + 4|t_{s\sigma}^{(0)}|^2}) / (2t_s + 2|t_{s\sigma}^{(0)}|)$. Therefore the two edge modes are polarized to the opposite $\pm x$ directions. Note that ψ_L and ψ_R span the complete Hilbert space of one single 1/2 spin or spin qubit. Each edge state equals one half of a single spin, similar to the relation between a Majorana fermion and a complex fermion in topological superconductors. As a result, we expect the robustness of the zero modes to any local operations without breaking the $U(1)$ and $\mathcal{C}\mathcal{T}$ symmetries [30]. These properties of the topological spin qubit (TSQ) may be applicable to fault-tolerant quantum computation [9]. Moreover, the Z classification implies that single-particle couplings respecting $U(1)$ and $\mathcal{C}\mathcal{T}$ cannot gap out the edge modes in an arbitrary N -chain system of 1D lattices. Interestingly, however, we have confirmed that with weak interactions a system with up to four chains of the 1D lattices can be adiabatically connected to a trivial phase without closing the bulk gap, implying that the Z

classification breaks down to Z_4 with the interactions [28]. This result suggests an interesting platform to study the classification of SPT phases with cold atoms.

The existence of zero modes leads to particle fractionalization, which is another direct observable in experiments. Note that a zero mode is equally contributed from the valence band and the conduction band. Therefore, an edge state carries a $+1/2$ ($-1/2$) particle if it is occupied (unoccupied) [28]. This result is confirmed by the numerical simulation shown in Fig. 2, where we calculate $\Delta N_{1,2}(x_i) = \int_0^{x_i} dx' N_{1,2}(x') - x_i/a$ at half filling, with $N_{1(2)}(x)$ the density of fermions when the left (right) edge mode is filled. The fermion number carried by an occupied (unoccupied) edge mode is then given by $n_{1(2)} = \Delta N_{1(2)}(\xi)$ with $\xi \gg \xi_0$. Here $\xi_0 = -a/\ln|\lambda_+|$ is the localization length of $\psi_{L,R}$. The $1/2$ fractionalization is clearly seen when ξ is several times greater than ξ_0 [see Fig. 2(b)]. Being a topological invariant, the $1/2$ fractionalization can be confirmed to be robust against weak disorder scatterings without breaking the given symmetries.

Correlation effects.—A particular advantage in cold atoms is that one can investigate correlation effects on the predicted SPT phase by precisely controlling the interaction. For spin-1/2 cold fermions the onsite Hubbard interaction $U\sum_i n_{i\uparrow}n_{i\downarrow}$ can be well controlled by the Feshbach resonance [27]. For a single-chain system, we expect that the topological phase is stable against weak interactions relative to the single-particle bulk gap, while the strong repulsive interaction can always drive the system into a Mott insulating phase. The correlation effects around the critical point can be probed by an Abelian bosonization approach combined with renormalization group (RG) analysis [31]. Note that in the noninteracting regime, the phase diagram of the single-chain system is determined by the SO and Zeeman terms which define two mass terms $\mathcal{H}_{SO} = \frac{u}{\pi a} \sin\sqrt{2}\phi_\rho \cos\sqrt{2}\theta_\sigma$, $\mathcal{H}_Z = \frac{w}{\pi a} \cos\sqrt{2}\phi_\rho \sin\sqrt{2}\theta_\sigma$ in the bosonized Hamiltonian, where the masses $u = 2t_{so}^{(0)}$ and $w = \Gamma_y$, and $\phi_{\rho,\sigma}$, $\theta_{\rho,\sigma}$ are the boson representations of the fermion fields [28]. The fate of the system in the presence of the interaction depends on which mass term flows first to the strong coupling regime under the RG.

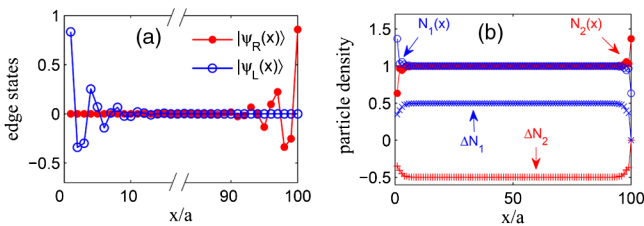


FIG. 2 (color online). (a) Wave functions for zero modes $|\psi_{L,R}\rangle$; (b) $1/2$ -particle fractionalization (seen by $\Delta N_{1,2}$) for zero modes. The parameters $t_{so}^{(0)} = 0.4t_s$ and $\Gamma_z = 0.3t_s$, with which the localization length of bound modes $\xi_0 = 2.36a$.

A direct power counting shows the same RG flow for the masses u and w in the first-order perturbation. Therefore the next-order perturbation expansion is necessary to capture correctly the fate of the topological phase transition. By deriving the RG flow equations up to one-loop order [32], we find the renormalization to u , w , the umklapp scattering g_ρ , and spin backscattering g_σ by [28]

$$\begin{aligned} \frac{du}{dl} &= \frac{3 - K_\rho}{2} u - \frac{g_\rho u}{4\pi v_F} + \frac{g_\sigma u}{4\pi v_F}, \\ \frac{dw}{dl} &= \frac{3 - K_\rho}{2} w + \frac{g_\rho w}{4\pi v_F} + \frac{g_\sigma w}{4\pi v_F}, \\ \frac{dg_\rho}{dl} &= \frac{g_\rho^2}{\pi v_F}, \quad \frac{dg_\sigma}{dl} = \frac{g_\sigma^2}{\pi v_F}, \end{aligned} \quad (4)$$

where the bare values of the coupling constants $g_\rho = -g_\sigma = U$, $u = 2t_{so}^{(0)}$, $w = \Gamma_y$, and l is the logarithm of the length scale. The renormalization of the Luttinger parameter K_ρ has been neglected as it is a higher order correction. For $U > 0$, g_σ marginally flows to zero so we drop it off below. This is consistent with the result that the repulsive interaction cannot gap out the spin sector in the 1D Hubbard model. g_ρ is marginally relevant and can be solved by $g_\rho(l) = \frac{\pi v_F g_\rho(0)}{\pi v_F - g_\rho(0)l}$. Substituting this result into the RG equations of u and w yields after integration $u(l) = u(0)[1 - \frac{g_\rho(0)l}{\pi v_F}]^{1/4} e^{(3-K_\rho)l/2}$, $w(l) = w(0)[1 + \frac{g_\rho(0)l}{\pi v_F}]^{1/4} e^{(3-K_\rho)l/2}$. The physics is clear: the repulsive interaction ($g_\rho > 0$) suppresses the SO induced mass term u while it enhances the trivial mass term w . The fate of the system depends on which of u and w reaches the strong-coupling regime first. Assuming $|g_\rho(0)l| \ll \pi v_F$, we find the TP transition occurs at

$$u(0) = [w(0)]^\gamma, \quad \gamma \approx 1 - \frac{g_\rho(0)}{4\pi v_F(3 - K_\rho)}. \quad (5)$$

This gives the scaling law at the phase boundary with the interaction. Note that $\gamma < 1$ for $U > 0$. The above scaling relation implies that a repulsive interaction suppresses the SPT phase. Accordingly, if initially the noninteracting system is topologically nontrivial with $u(0) > w(0) > 0$, increasing U to the regime $u(0) < [w(0)]^\gamma$ drives the system into a trivial phase.

Single spin control.—Now we study an interesting application of the present results to realizing single spin control. Besides the edge modes localized on the ends, TSQs can also be obtained in the middle areas by creating mass domains in the lattice. This can be achieved by applying a local Zeeman term Γ_y or Γ_z . For example, we consider $\Gamma_z = 0$ everywhere, but $\Gamma_y = \Gamma_0$ for $x_1 < x < x_2$ and $\Gamma_y = 0$ otherwise. The local Γ_y can be generated by applying another two lasers which cross with the 1D lattice and couple the atoms in the area $x_1 < x < x_2$ to induce a local resonant Raman coupling between $|g_\uparrow\rangle$ and $|g_\downarrow\rangle$ [see Fig. 3(a)]. Employing a $\pi/2$ -phase offset in the Rabi

frequencies of the two lasers, the Raman coupling takes the form $\Gamma_0 \sigma_y$, with Γ_0 controlled by the laser strength. When $|\Gamma_0| > 2|t_{\text{so}}^{(0)}|$ a mass domain is created, associated with two midgap spin states $|\psi_{\pm}\rangle$ respectively localized around $x = x_{1,2}$ [see Fig. 3(a)]. The width $\Delta x = x_2 - x_1$ and height of the domain are respectively adjusted by the waist size and strength of the two laser beams. Due to the nonlocality of the TSQ, the creation of a single qubit here is not restricted by the size of the laser beams. This is a fundamental difference from creating a conventional single qubit by optical dipole trapping which requires tiny-sized laser beams to reach a very small trapping volume [33]. Note in the realistic case that the laser induced Γ_y may vary fast but not in the form of step functions around $x = x_{1,2}$, which, however, does not affect the main results presented here [28]. Coupling between $|\psi_{+}\rangle$ and $|\psi_{-}\rangle$ results in an energy splitting $2\mathcal{E} \propto e^{-(|\Gamma_0| - 2|t_{\text{so}}^{(0)}|)\Delta x/(2at_s)}$, which is controlled by Γ_0 and Δx [see Fig. 3(a), lower panel]. In the limit $(|\Gamma_0| - 2|t_{\text{so}}^{(0)}|)\Delta x/(2at_s) \gg 1$, such coupling is negligible, and the two zero modes consist of a single spin qubit which is topologically stable. Let $|\psi_{+}\rangle$ be initially occupied while $|\psi_{-}\rangle$ is left vacant. Reducing $|\Gamma_0|$ smoothly can open the coupling in $|\psi_{\pm}\rangle$ and lead to the spin state evolving as [34] $|\psi(t)\rangle = \alpha(t)\varphi_{-}(x-x_1)|\chi_{-}\rangle + \beta(t)\varphi_{+}(x-x_2)|\chi_{+}\rangle$, with $\alpha(0) = 0$, $\beta(0) = 1$, and φ_{\pm} the spatial parts of the bound state wave functions. The spin-polarization densities are given by $s_{x,y,z}(x,t) = \langle \psi(x) | \sigma_{x,y,z} | \psi(x) \rangle$, and the spin expectation values

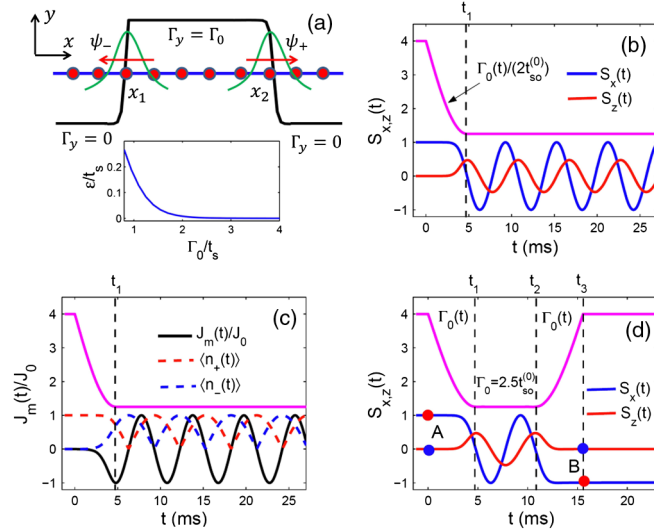


FIG. 3 (color online). Spin Rabi oscillations with the parameters $t_s = 3.15$ kHz, $t_{\text{so}}^{(0)} = 0.4t_s$, and $\Delta x = 10a \sim 4 \mu\text{m}$. (a) Mass domain created by setting $|\Gamma_0| > 2t_{\text{so}}^{(0)}$ for $x_1 < x < x_2$ which localizes a spin qubit composed of two bound modes $|\psi_{\pm}\rangle$ on $x = x_1, x_2$, respectively. (b) Spin Rabi oscillation by smoothly reducing $|\Gamma_0|$ from $8t_{\text{so}}^{(0)}$ to $2.5t_{\text{so}}^{(0)}$. (c) The mass current $J_m(t)$ and expectation values of particle numbers $\langle n_{\pm}(t) \rangle$ in states $|\psi_{\pm}\rangle$. (d) Spin-flip operation by controlling $\gamma(t_3) = (2m + 1)\pi$ with $m = 1$. The initial spin state $|\chi_{+}\rangle$ (points A) flips to be $|\chi_{-}\rangle$ (points B).

$S_{x,y,z}(t) = \int dx s_{x,y,z}(x,t)$. It can be verified that $S_y(t) = 0$, and

$$S_x(t) = |\alpha(t)|^2 - |\beta(t)|^2,$$

$$S_z(t) = 2\text{Re}[\alpha(t)\beta^*(t) \int dx \varphi_{+}^*(x)\varphi_{-}(x)]. \quad (6)$$

This phenomenon is analogous to spin precession with the rotating angle yielding $\gamma(t) = 2 \int_0^t dt' \mathcal{E}(t')$. We have then $\alpha = \cos\gamma(t)$ and $\beta = \sin\gamma(t)$. The amplitude of $S_z(t)$ is given by $S_z^{\text{max}} = |\int dx \varphi_{+}^*(x)\varphi_{-}(x)|$, which measures the overlapping integral of φ_{\pm} . Accordingly, if we apply the local Zeeman field along the z axis rather than the y axis, we shall obtain that the spin evolves in the xy plane. Note that the spin Rabi oscillation is induced by quantum tunneling. Therefore it is associated with a tunneling current given by $J_m(t) = -\frac{\Delta x \mathcal{E}}{2\pi\hbar} \partial_t |\alpha(t)|^2$ between x_1 and x_2 . In experiments the internal states of a single atom can be detected without energy transfer [35], which is applicable to observations of the spin Rabi oscillations, while the oscillation of $S_x(t)$ can be more conveniently observed by measuring the number of fermions $\langle n_{\pm}(t) \rangle$ localized around $x_{1,2}$ with single-site resolution technology [36], and $J_m(t)$ can be detected by measuring the change rate with time of such fermion numbers.

We show in Figs. 3(b)–3(d) the numerical simulation for single spin control with the parameter regime $t_s = 3.15$ kHz, $t_{\text{so}}^{(0)} = 0.4t_s$, and $\Delta x = 10a$. For $t < 0$, $\Gamma_0 = 8t_{\text{so}}^{(0)}$ and the coupling in $|\psi_{\pm}\rangle$ is negligible. Reducing Γ_0 at $t > 0$ leads to spin evolution and by fixing $\Gamma_0 = 2.5t_{\text{so}}^{(0)}$ for $t > t_1$ the spin oscillates with a period of 5.984 ms [see Figs. 3(b) and 3(c)]. Note that the quantum state of the spin can be precisely controlled by properly manipulating $\gamma(t)$. For example, in Fig. 3(d) we demonstrate the spin-flip operation $|\chi_{+}\rangle \rightarrow |\chi_{-}\rangle$ by requiring $\gamma(t_3) = (2m + 1)\pi$. Here $m \in \mathbb{Z}$ and in Fig. 3(d) we take $m = 1$. Note that one may integrate multiple TSQs with, e.g., atom-chip technology, and individually control them by creating multiple mass domains in the 1D lattice. The precise manipulation of such integrated TSQs may have interesting applications in developing scalable spin-based quantum computers.

Finally we estimate the parameter values for realistic experimental observations. For example, in 40 K atoms we have the recoil energy $E_R/\hbar = \hbar k_0^2/2m = 48$ kHz using red-detuned lasers of wavelength 773 nm to form the optical lattice. Taking $V_0 = 5E_R$ and $M_0 = 2E_R$, we have the lattice trapping frequency $\omega = 214$ kHz, and hopping coefficients $t_s/\hbar \approx 3.15$ kHz and $t_{\text{so}}^{(0)}/\hbar \approx 1.3$ kHz. Then the bulk gap equals $E_g/\hbar = 2.6$ kHz for $\Gamma_z = 0$, indicating a temperature $T = 19$ nK for the experimental observation. Also, under this parameter regime the lifetime of the atoms is over 1.0 s, which is long enough for the detection and manipulation of the topological edge spins.

Conclusions.—We have proposed to observe and manipulate the SPT phase of the AIII class in a 1D optical lattice, and have demonstrated single spin control by

manipulating spin-polarized zero modes which is applicable to spin-based quantum computation. The minimum requirement for the proposed scheme is a regular 1D lattice and a transverse Zeeman field, which can be realized simultaneously in a single two-photon Raman transition as used in the recent experiments [11–15]. The present study may open the search for topological states of all ten Altland-Zirnbauer symmetry classes with realistic cold atom systems, and its remarkable feasibility will attract both theoretical and experimental efforts in the future.

We thank T.-L. Ho, X. G. Wen, X. Chen, V. W. Liu, and C. Xu for helpful discussions. We thank the support of JQI-NSF-PFC, Microsoft-Q, and DARPAQuEST. X.-J. L. also thanks the support from HKRGC through Grants No. 605512 and No. HKUST3/CRF0. Z. X. L. thanks the support from NSFC 11204149.

-
- [1] K. V. Klitzing, G. Dorda, and M. Pepper, *Phys. Rev. Lett.* **45**, 494 (1980); D. C. Tsui, H. L. Stormer, and A. C. Gossard, *Phys. Rev. Lett.* **48**, 1559 (1982).
- [2] F. D. M. Haldane, *Phys. Rev. Lett.* **50**, 1153 (1983); *Phys. Lett.* **93**, 464 (1983); N. Read and D. Green, *Phys. Rev. B* **61**, 10267 (2000); A. Y. Kitaev, *Phys. Usp.* **44**, 131 (2001).
- [3] C. L. Kane and E. J. Mele, *Phys. Rev. Lett.* **95**, 146802 (2005); B. A. Bernevig, T. L. Hughes, and S.-C. Zhang, *Science* **314**, 1757 (2006); L. Fu, C. L. Kane, and E. J. Mele, *Phys. Rev. Lett.* **98**, 106803 (2007); J. E. Moore and L. Balents, *Phys. Rev. B* **75**, 121306(R) (2007); R. Roy, *ibid.* **79**, 195322 (2009).
- [4] M. Z. Hasan and C. L. Kane, *Rev. Mod. Phys.* **82**, 3045 (2010); X.-L. Qi and S.-C. Zhang, *ibid.* **83**, 1057 (2011).
- [5] A. Altland and Martin R. Zirnbauer, *Phys. Rev. B* **55**, 1142 (1997).
- [6] Z. C. Gu and X. G. Wen, *Phys. Rev. B* **80**, 155131 (2009); X. Chen, Z.-C. Gu, and X.-G. Wen, *ibid.* **82**, 155138 (2010); X.-G. Wen, *ibid.* **85**, 085103 (2012).
- [7] S. Ryu, A. P. Schnyder, A. Furusaki, and A. W. W. Ludwig, *New J. Phys.* **12**, 065010 (2010).
- [8] L. Fidkowski and A. Kitaev, *Phys. Rev. B* **81**, 134509 (2010); A. M. Turner, F. Pollmann, and E. Berg, *ibid.* **83**, 075102 (2011); L. Fidkowski and A. Kitaev, *ibid.* **83**, 075103 (2011).
- [9] Y. Kitaev, *Ann. Phys. (Amsterdam)* **303**, 2 (2003); S. Das Sarma, M. Freedman, and C. Nayak, *Phys. Rev. Lett.* **94**, 166802 (2005); C. Nayak, A. Stern, M. Freedman, and S. D. Sarma, *Rev. Mod. Phys.* **80**, 1083 (2008).
- [10] X.-J. Liu, M. F. Borunda, X. Liu, and J. Sinova, *Phys. Rev. Lett.* **102**, 046402 (2009).
- [11] Y.-J. Lin, K. Jiménez-García, and I. B. Spielman, *Nature (London)* **471**, 83 (2011).
- [12] M. Chapman and C. Sá de Melo, *Nature (London)* **471**, 41 (2011).
- [13] P. Wang, Z.-Q. Yu, Z. Fu, J. Miao, L. Huang, S. Chai, H. Zhai, and J. Zhang, *Phys. Rev. Lett.* **109**, 095301 (2012).
- [14] L. W. Cheuk, A. T. Sommer, Z. Hadzibabic, T. Yefsah, W. S. Bakr, and M. W. Zwierlein, *Phys. Rev. Lett.* **109**, 095302 (2012).
- [15] J.-Y. Zhang *et al.*, *Phys. Rev. Lett.* **109**, 115301 (2012).
- [16] J. Larson, J.-P. Martikainen, A. Collin, and E. Sjöqvist, *Phys. Rev. A* **82**, 043620 (2010); D. Sokolovski and E. Ya. Sherman, *ibid.* **84**, 030101(R) (2011); J. D. Sau, R. Sensarma, S. Powell, I. B. Spielman, and S. Das Sarma, *Phys. Rev. B* **83**, 140510(R) (2011); T. Ozawa and G. Baym, *Phys. Rev. Lett.* **109**, 025301 (2012); G. I. Martone, Y. Li, L. P. Pitaevskii, and S. Stringari, [arXiv:1207.6804](https://arxiv.org/abs/1207.6804).
- [17] X.-J. Liu, X. Liu, L. C. Kwek, and C. H. Oh, *Phys. Rev. Lett.* **98**, 026602 (2007); *Phys. Rev. B* **79**, 165301 (2009).
- [18] C. Wu, *Phys. Rev. Lett.* **101**, 186807 (2008); X.-J. Liu, X. Liu, C. Wu, and J. Sinova, *Phys. Rev. A* **81**, 033622 (2010); Y. Yu and K. Yang, *Phys. Rev. Lett.* **105**, 150605 (2010).
- [19] N. Goldman, I. Satija, P. Nikolic, A. Bermudez, M. A. Martin-Delgado, M. Lewenstein, and I. B. Spielman, *Phys. Rev. Lett.* **105**, 255302 (2010); N. Goldman, J. Beugnon, and F. Gerbier, *ibid.* **108**, 255303 (2012).
- [20] X. Li, E. Zhao, and V. W. Liu, [arXiv:1205.0254](https://arxiv.org/abs/1205.0254).
- [21] G. Liu, S.-L. Zhu, S. Jiang, F. Sun, and W. M. Liu, *Phys. Rev. A* **82**, 053605 (2010); F. Mei, S.-L. Zhu, Z.-M. Zhang, C. H. Oh, and N. Goldman, *ibid.* **85**, 013638 (2012).
- [22] C. Zhang, S. Tewari, R. M. Lutchyn, and S. Das Sarma, *Phys. Rev. Lett.* **101**, 160401 (2008); Y. Zhang, L. Mao, and C. Zhang, *ibid.* **108**, 035302 (2012).
- [23] M. Sato, Y. Takahashi, and S. Fujimoto, *Phys. Rev. Lett.* **103**, 020401 (2009).
- [24] S.-L. Zhu, L. B. Shao, Z. D. Wang, and L.-M. Duan, *Phys. Rev. Lett.* **106**, 100404 (2011); W. Yi and G.-C. Guo, *Phys. Rev. A* **84**, 031608(R) (2011); L. He and X.-G. Huang, *Phys. Rev. Lett.* **108**, 145302 (2012); *Phys. Rev. B* **86**, 014511 (2012).
- [25] Kangjun Seo, Li Han, and C. A. R. Sá de Melo, *Phys. Rev. Lett.* **109**, 105303 (2012).
- [26] C. V. Kraus, S. Diehl, P. Zoller, and M. A. Baranov, [arXiv:1201.3253](https://arxiv.org/abs/1201.3253); S. Nascimbè, [arXiv:1210.0687](https://arxiv.org/abs/1210.0687).
- [27] I. Bloch, J. Dalibard, and W. Zwerger, *Rev. Mod. Phys.* **80**, 885 (2008).
- [28] See Supplemental Material at <http://link.aps.org/supplemental/10.1103/PhysRevLett.110.076401> for details.
- [29] T. P. Meyrath, F. Schreck, J. L. Hanssen, C.-S. Chuu, and M. G. Raizen, *Phys. Rev. A* **71**, 041604(R) (2005).
- [30] Note that the degeneracy and spin polarization of the edge modes obtained by F. Mei *et al.* in Ref. [21] are not symmetry protected and not stable against local perturbations. Therefore such edge modes cannot form TSQs.
- [31] T. Giamarchi, *Quantum Physics in One Dimension* (Oxford University Press, New York, 2004).
- [32] L. Balents and M. P. A. Fisher, *Phys. Rev. B* **53**, 12133 (1996).
- [33] N. Schlosser, G. Reymond, I. Protsenko, and P. Grangier, *Nature (London)* **411**, 1024 (2001).
- [34] We neglect the couplings between $|\psi_{\pm}\rangle$ and the bulk states $|u_k\rangle$, which is valid when $|\langle\psi_{\pm}|\partial_t|u_k\rangle| \ll E_g$ during the manipulation.
- [35] J. Volz, R. Gehr, G. Dubois, J. Estève, and J. Reichel, *Nature (London)* **475**, 210 (2011).
- [36] W. S. Bakr, J. I. Gillen, A. Peng, S. Foelling, and M. Greiner, *Nature (London)* **462**, 74 (2009); M. Karski, L. Förster, J. M. Choi, W. Alt, A. Widera, and D. Meschede, *Phys. Rev. Lett.* **102**, 053001 (2009).